

# Rapid penetration of bismuth from solid $\text{Bi}_2\text{Te}_3$ along grain boundaries in Cu and Cu-based alloys

S. N. Zhevnenko · D. V. Vaganov · E. I. Gershman

Received: 18 August 2010/Accepted: 30 December 2010/Published online: 21 January 2011  
© Springer Science+Business Media, LLC 2011

**Abstract** As well known, bismuth rapidly penetrates into copper grain boundaries at about 550 °C and embrittles copper. In the experiments, the authors have used solid  $\text{Bi}_2\text{Te}_3$  for the embrittlement of pure copper and copper-based solid solutions containing iron and silver. The investigated alloys were heated in the closed volume together with  $\text{Bi}_2\text{Te}_3$  for a short time (5–90 min) at 570 °C in the hydrogen atmosphere.  $\text{Bi}_2\text{Te}_3$  did not contact with copper samples during annealing. After that, the samples were bent and grain boundary cracks were formed (with the depth about 10–500 μm). Experiment showed that silver accelerates the embrittlement in the contrast to iron. The cracks in the silver–copper alloys were deeper than in the iron–copper ones. It was assumed that the depth of cracks is equal to the penetration depth. The reasons for this phenomenon were discussed in terms of the impurities effect on the grain boundary segregation.

## Introduction

A liquid metal which contacts a solid metal can rapidly penetrate into grain boundaries of the solid. The rapid liquid metal penetration (LMP) can proceed in the presence or absence of external stresses. Liquid metal penetration under applied stresses is well known and good theoretical models of this process are worked out [1–7]. The special couples of metals like Al–Ga, Cu–Bi, and Ni–Bi are most interesting because in this case, LMP occurs without external stresses.

As it is well known, LPM has three stages (Fig. 1a). The first stage is the liquid metal grooving [8], the second stage is the liquid metal penetration along the thick channel (with thickness about 1 μm) and the third stage is the penetration along the thin channel (about 10 nm thick) [7]. The most interesting stage is the third one. There is no clear understanding of the penetration mechanism. The kinetics of the thin channel penetration had not been experimentally investigated (to the best of our knowledge).

In the recent article [9], the authors described the experiment which allowed separating the stage of a thin channel penetration in the Cu–Bi system using the chemical compound  $\text{Bi}_2\text{Te}_3$ . The main idea of this experiment was to restrict the amount of Bi on the copper free surface. It is different in comparison to usual experiments where the amount of liquid bismuth on the surface of a polycrystal is unlimited. The  $\text{Bi}_2\text{Te}_3$  compound decomposes at 570 °C that makes possible to expose a Cu-based polycrystal to the Bi-containing gas atmosphere above 570 °C. In these conditions, bismuth is deposited onto the free surface of the sample from the gas phase and penetrates into the grain boundaries of copper polycrystal. The preliminary experiments have shown that the liquid metal grooving and wide penetration channels are absent in such conditions. The authors suppose to be able to separate only the stage of thin channel penetration. In this study, the effect of Fe and Ag on the grain boundary liquid bismuth penetration in Cu from the  $\text{Bi}_2\text{Te}_3$  source has been studied.

## Experimental

Polycrystalline copper of 99.99 wt% purity was used for this investigation. Silver and iron (purity 99.95 wt%) were used to prepare Cu–1.4 at.%Ag and Cu–0.4 at.%Fe solid

S. N. Zhevnenko (✉) · D. V. Vaganov · E. I. Gershman  
Department of Physical Chemistry, National University  
of Science and Technology “MISIS”, Leninsky pr. 4,  
Moscow 119049, Russia  
e-mail: zhevnenko@misis.ru

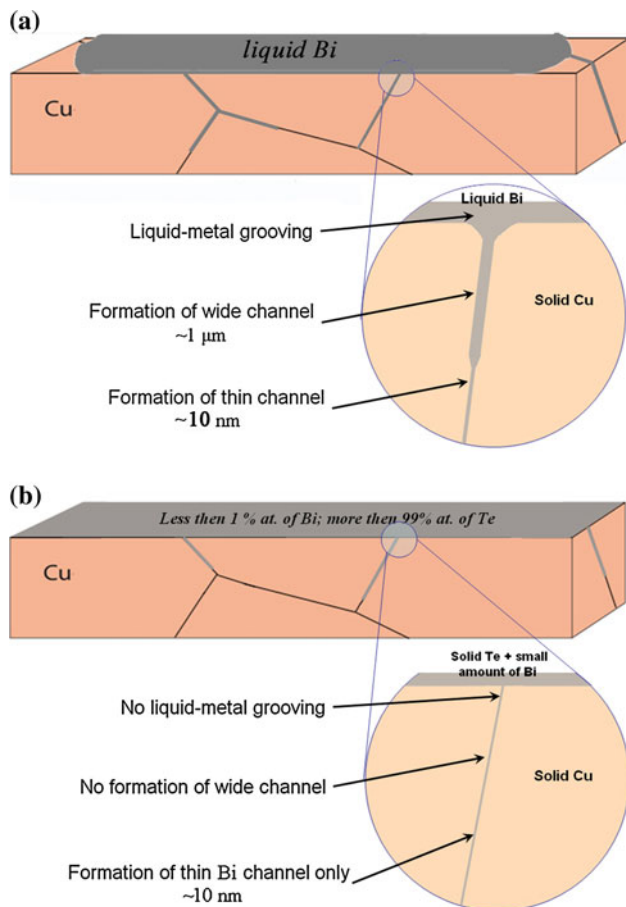


**Fig. 1** Scheme of classical liquid metal penetration (a) and scheme of liquid metal penetration in present work (b)

solutions. The ingots were cut into  $(15 \times 3 \times 1)$  mm plates. Each specimen was polished and annealed for 2 h at  $1000^{\circ}\text{C}$  in  $\text{H}_2$  atmosphere to perform homogenization, recrystallization, and stabilization of the structure.

The annealing with  $\text{Bi}_2\text{Te}_3$  was performed for 10–90 min at  $570^{\circ}\text{C}$  in  $\text{H}_2$  atmosphere. The chamber with the samples was put into the heated furnace. Heating time of the chamber is comparable with the time of the experiments. Therefore, the time dependence of the chamber temperature during the heating was measured before the actual experiments. During the experiments, the samples and a piece of  $\text{Bi}_2\text{Te}_3$  were held in a special quartz holder. Specimens and  $\text{Bi}_2\text{Te}_3$  were not in the contact. The chamber was blown by argon and hydrogen before being placed in the furnace.

After the annealing the surface of all samples appeared to be covered by a thin layer of  $\text{Bi}_2\text{Te}_3$  decay products. This surface layer contained more than 99 at.% Te and less than 1% Bi. At the same time,  $\text{Bi}_2\text{Te}_3$  remained solid (Fig. 2). Melting point of bismuth telluride is  $586^{\circ}\text{C}$ . Specimens were curved after annealing with  $\text{Bi}_2\text{Te}_3$ . Along

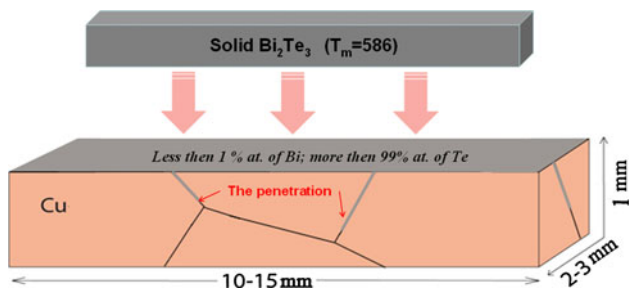


**Fig. 2** Scheme of experiment in this study

the grain boundaries cracks formed starting from the surface. The cracks were directed into the core of the specimens. It was found that, with the microanalysis, the average Bi penetration depth is equal to the average cracks length. Every average penetration depth value was obtained from 30 to 40 crack measurements.

## Results and discussion

Grain boundary brittle cracks appear already after 10 min of annealing. At this moment, the chamber reached the temperature of  $550^{\circ}\text{C}$  (Fig. 3). On the other hand, the decay products appeared on the surface of the sample before 10 min of annealing. Therefore, the Bi penetration starts at about  $550^{\circ}\text{C}$ . The time dependence of Bi penetration is parabolic. The penetration curve has been straightened in logarithmical coordinates to get the kinetics exponent. The kinetics exponent for penetration in grain boundaries of pure copper is  $\sim 0.5$  (Fig. 4a).

The value of the kinetics exponent (0.5) permits to suppose that the Bi penetration process is diffusion-controlled.

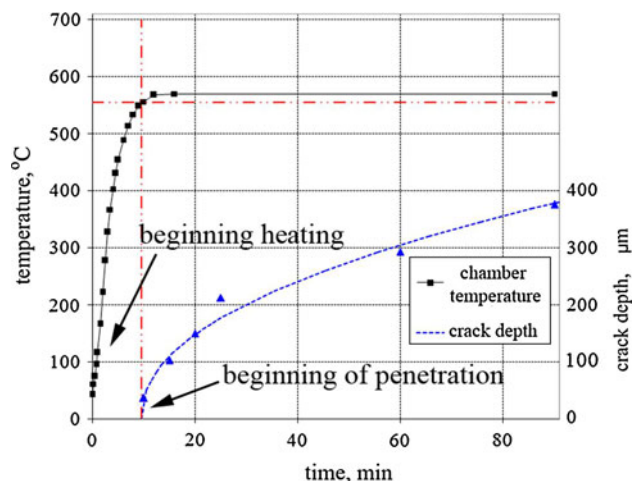


**Fig. 3** The time dependence of the average crack depth for pure copper

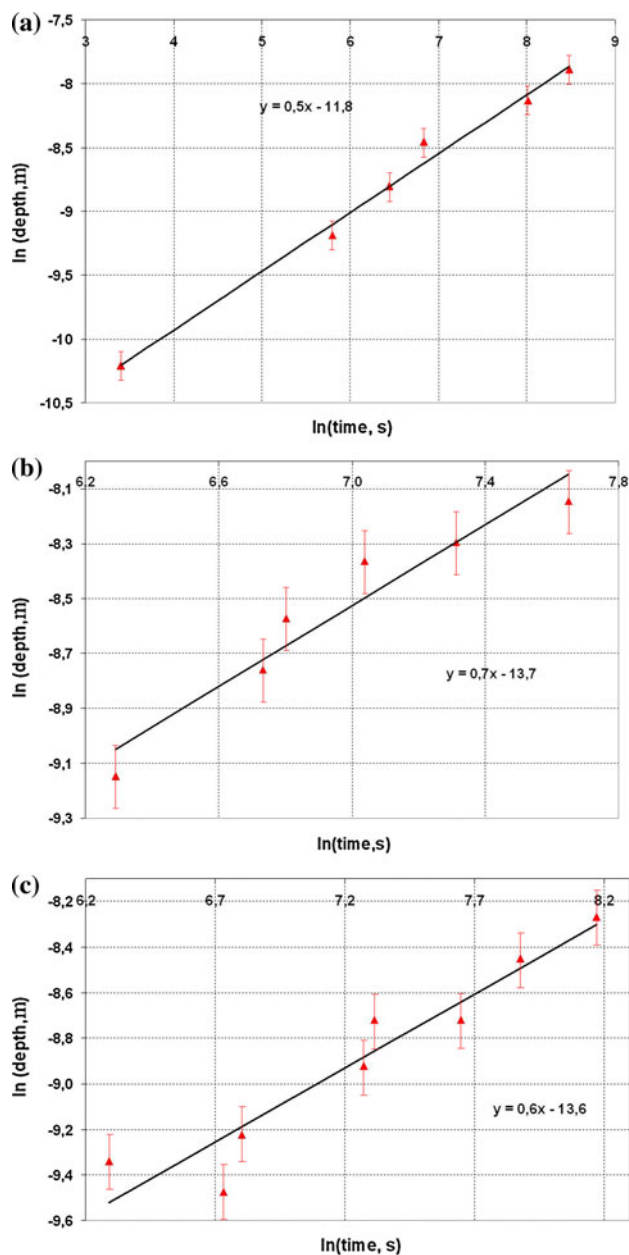


**Fig. 4** The time dependences of penetration depth in pure copper (a), in solid solution Cu-1.4 at.%Ag (b) and in solid solution Cu-0.4 at.%Fe (c) in logarithmical coordinates

It should be noted that penetration rate is close to the grain boundary diffusion rate of the pure bismuth in copper. Grain boundary diffusion coefficient of bismuth in pure copper is extrapolated from diffusion the data [10] and it is  $5 \times 10^{-11} \text{ m}^2/\text{s}$  at 570 °C. Roughly estimating the diffusion path as  $\sqrt{D_{\text{GBT}} t}$ , it is possible to calculate the penetration depth which is about 500 μm for the 1.5 h of annealing time. This value is close to the penetration depth measured in the present work (400 μm).

#### Auger electron spectroscopy of brittle fracture surfaces of pure Cu

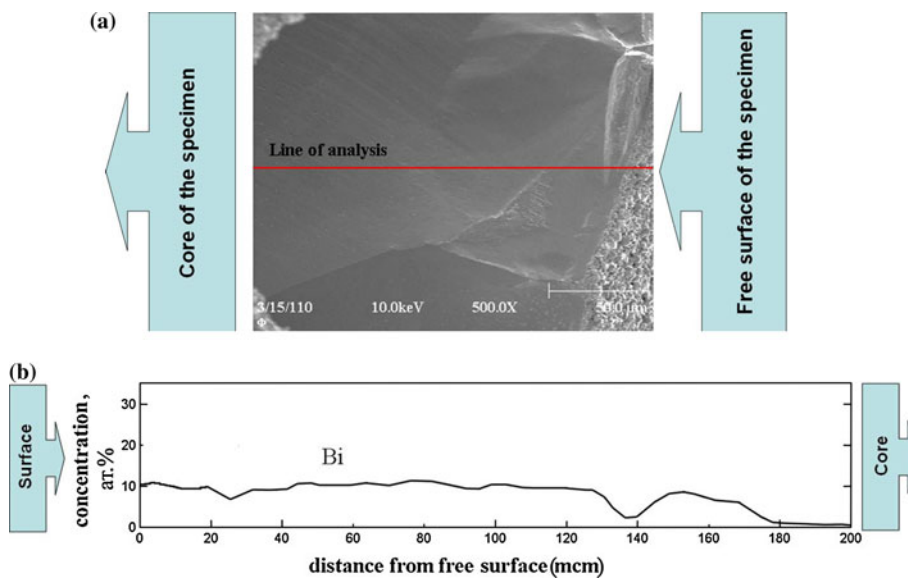
The embrittled sample of pure copper was broken in the preparation chamber of Auger spectroscopic microscope and the surface of grain boundary brittle fractures were investigated. The lateral analysis of bismuth amount shows uniform distribution of bismuth on the grain boundary fracture surface (Fig. 5). The bismuth concentration falls down to the background level after the layer of about 5–10 nm thickness has been sputtered by an ion beam [9]. The fact of uniform Bi distribution on the grain boundary fracture surfaces permits to suppose that there is a *liquid* metal penetration. As the authors assumed, the liquid metal penetration in this study occurs without formation of wide channels and liquid metal grooves (Fig. 1b).

It would be noted that the described process of bismuth penetration into the copper grain boundaries is not in equilibrium. After the replacing of Bi source from the copper free surface and further annealing at the same temperature, the copper samples are getting back ductile. In other words, bismuth is leaving the grain boundaries after annealing without its source. Bismuth layers on the copper grain boundaries are not equilibrium in these experiments. It is the main difference from grain boundary wetting experiments [11–13].

There are three facts which can be used for discussion of the possible penetration mechanism. The first fact is parabolic time dependence of penetration depth. The second fact is the uniform Bi distribution on the grain boundary fracture surfaces. And the third fact is the absence of tellurium on the grain boundary fracture surfaces. At the same time, there is a considerable amount of tellurium on the free surface of the sample.

The second fact indicates the presence of the liquid phase. The diffusion in the liquid phase is much faster than diffusion in grain boundary at the temperature of the experiment. It explains the uniform Bi distribution on the grain boundary fracture surfaces. Did the penetrated liquid form on the free surface and then penetrated into a grain boundary or did it form directly inside the grain boundary? The absence of tellurium in the grain boundary leads to the second answer. Finally, why the kinetic curve is parabolic with 0.5 kinetics exponent? Where could diffusion proceed? It is possible to expect the following penetration mechanism. Bismuth penetrates into the grain boundary by the diffusion on short distance. It leads to the liquid phase formation. Liquid provides the fast way for the supply of bismuth from the free surface. Assuming that the limiting stage of a process is the diffusion into the grain boundary we can explain the parabolic time dependence. Molar volume of the liquid bismuth is less than that of the molar

**Fig. 5** Auger analysis of bismuth lateral distribution on the grain boundary brittle fracture surface **a** SEM of the brittle fractured grain boundary. **b** Bi concentration as a function of the distance from free surface



volume of solid bismuth ( $20.8 \text{ cm}^3/\text{mol}$  for liquid bismuth and  $21.5 \text{ cm}^3/\text{mol}$  for solid bismuth at the melting point [14]) so there is no flux of the matter from the penetration channel if the formed Bi–Cu liquid has the higher density than corresponding solid phase.

In the authors' opinion, the penetration mechanism can be qualitatively explained as follows. Bismuth penetrates into the copper grain boundary by diffusion. When the grain boundary concentration of bismuth becomes sufficient, the grain boundary area melts. After that the transport of bismuth into the grain boundary is carried out by the diffusion in the liquid phase. The melted matter has volume less or equal to that of the corresponding solid phase. As a result there is no extrusive flux. It should be noted that the gallium also melts with decreasing volume ( $11.5 \text{ cm}^3/\text{mol}$  for liquid gallium and  $11.8 \text{ cm}^3/\text{mol}$  for solid gallium [14]) and phenomenon of LMP without external stresses in the Al–Ga system is very well known [15–17]. Other systems that demonstrate such behavior are Sn and Zn in Fe–Si [18]. Silicon is an element of reducing shrinkage cavity in iron alloys and silicon also melts with decreasing volume ( $11.2 \text{ cm}^3/\text{mol}$  for liquid silicon and  $12.1 \text{ cm}^3/\text{mol}$  for solid [14]).

#### Grain boundary penetration of Bi into the Cu–Ag and Cu–Fe solid solutions

On Fig. 4b, c the plots similar to that of Fig. 4a are presented for the Cu–1.4 at.%Ag and Cu–0.4 at.%Fe solid solutions, respectively. The samples were annealed at  $700^\circ\text{C}$ , 10 h before penetration procedure. The kinetics exponents are about 0.5 for both cases.

It appeared that silver increases the penetration rate and iron decreases. Silver in copper is the segregating impurity in contrast to the iron which is non-segregating impurity

[19]. This follows from the type of phase diagram. Eutectic type of phase diagram leads to segregation of impurity which enriches liquid phase. The liquid phase is depleted by the solute component in case of peritectic phase diagram. Therefore, the increase of penetration ratio can be explained by the decrease of the melting point of the penetrating liquid phase due to the silver segregation on the grain boundaries of copper. The situation is different in case of Cu–Fe solid solution. There is the increase of the melting temperature with increasing iron content as it follows from peritectic type of phase diagram. In the authors' understanding, it is the reason for the decrease of penetration ratio.

#### Auger electron spectroscopy of brittle fracture surfaces of Cu–Ag and Cu–Fe solid solutions

Auger electron spectroscopy of brittle fracture surfaces of Cu-based solid solution was performed. The temperature of the annealing for segregation was  $700^\circ\text{C}$ . Duration of the embrittlement was 15 min at  $570^\circ\text{C}$ . As expected, in the case of Cu–Ag solid solution, there is only a little enrichment of the grain boundary by Ag. The enrichment ratio is about 3.5 (Fig. 6b). It was obtained as a ratio of bismuth concentrations on the "fresh" fractured surface and after the layer of thickness about 50 nm was sputtered by the ion beam. This value is close to the calculated values for grain boundaries  $\Sigma = 5$  (310) at  $1200\text{ K}$  and  $\Sigma = 3$  (112) at  $750\text{ K}$  [20]. Authors of [21] estimated the segregation factor by the comparison of grain boundary diffusion coefficient at B and C regimes. Estimated segregation factor has the same order of magnitude as that in present work.

Auger analysis of Cu–0.4 at.%Fe brittle fracture shows the presence of precipitates on the grain boundary (Fig. 7a).

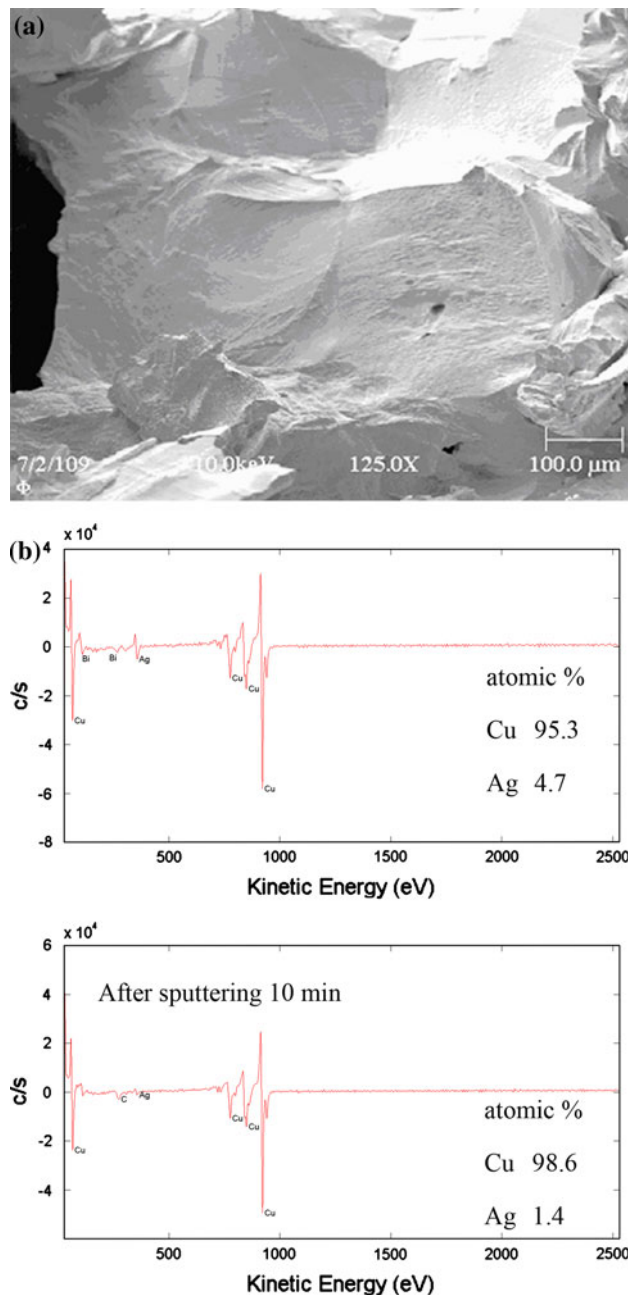


**Fig. 6** Brittle fracture of the Cu–1.4 at.%Ag sample (a) and Auger spectra from the splitted grain boundary before and after ion beam sputtering (b)

Precipitates have been observed in Cu–1.4 wt%Fe–0.6 wt%Co system before [22] but they were made by aging. The precipitates are enriched by iron (Fig. 7 b) and their average diameter is about 40 nm. At the same time the precipitate-free area has no significant concentration of iron. So in the author's opinion, the penetration rate of Bi on the precipitate-free area is close to the penetration rate along the grain boundary of pure copper. The precipitates on the grain boundaries occupy some area which can be

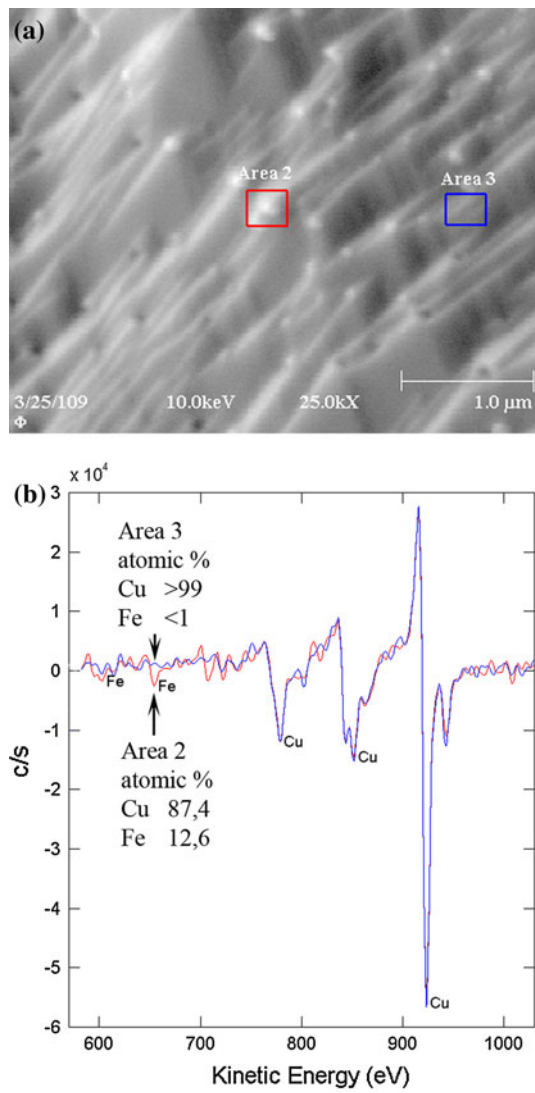


**Fig. 7** Brittle fracture of the Cu–0.4 at.%Fe sample (a) and Auger spectra of precipitate's area and precipitate-free area (b)

estimated at about 5 percent. Therefore, the rate of penetration decreases.

## Summary

Main conclusions are the following

- The thin channel penetration of bismuth from bismuth telluride into the grain boundaries of copper and copper-based solid solutions was demonstrated.
- The time dependence of the penetration depth is parabolic and the kinetics exponent is about 0.5.
- It was found that the presence of silver in copper increases the penetration rate; however, iron decreases this rate.

- The small positive segregation of silver on grain boundary Cu–1.4 at.%Ag solid solution was observed. The value of the enrichment ratio is about 3.5 at 700 °C.
- The precipitates on the grain boundary of Cu–0.4 at.%Fe were found.

## References

1. Nicholas MG, Old CF (1979) J Mater Sci 14:1. doi:[10.1007/BF01028323](https://doi.org/10.1007/BF01028323)
2. Glikman EE, Goryunov YV, Ledovskaya IY (1979) Sov Mater Sci 15:446
3. Joseph B, Barbier F, Dagoury G, Aucouturier M (1998) Scr Mater 39:775
4. Joseph B, Barbier F, Aucouturier M (1999) Scr Mater 40:893
5. Marie N, Wolski K, Biscondi M (2000) Scr Mater 43:943
6. Marie N, Wolski K, Biscondi M (2001) J Nucl Mater 296:282
7. Wolski K, Laporte V (2008) Mater Sci Eng A 495:138
8. Bokstein BS, Klinger LM, Apikhtina IV (1995) Mater Sci Eng A 203:373
9. Zhevnenko SN, Vaganov DV, Gershman EI (2010) Def Dif Forum 301:439
10. Divinski S, Lohmann M, Herzig C (2004) Acta Mater 52:3973
11. Straumal BB, Baretzky B, Kogtenkova OA, Straumal AB, Sidorenko AS (2010) J Mater Sci 45:2057. doi:[10.1007/s10853-009-4014-6](https://doi.org/10.1007/s10853-009-4014-6)
12. Straumal BB, Kogtenkova OA, Straumal AB, Kucheyev YuO, Baretzky B (2010) J Mater Sci 45:4271. doi:[10.1007/s10853-010-4377-8](https://doi.org/10.1007/s10853-010-4377-8)
13. Baram M, Kaplan DW (2006) J Mater Sci 41:7775. doi:[10.1007/s10853-006-0897-7](https://doi.org/10.1007/s10853-006-0897-7)
14. Gale WF, Totemeier TC (eds) (2004) Smithells metals reference book, 8th edn. Elsevier, Amsterdam
15. Ludwig W, Bellet D (2000) Mater Sci Eng A 281:198
16. Ludwig W, Pereiro-López E, Bellet D (2005) Acta Mater 53:151
17. Hugo RC, Hoagland RG (2000) Acta Mater 48:1949
18. Rabkin EI, Semenov VN, Shvindlerman LS, Straumal BB (1991) Acta Metall Mater 39:627
19. Gupta D (2003) Interface Sci 11:7
20. Menyhard M, Min Yan, Vitek V (1994) Acta Metall Mater 42:2783
21. Divinski S, Lohmann M, Herzig C (2001) Acta Mater 49:249
22. Monzen R, Echigo T (1999) Scr Mater 40:963